Proceedings World Geothermal Congress 2020+1
Reykjavik, Iceland, April - October 2021

Modelling of Fractured Granitic Geothermal Reservoirs: Use of Deterministic and stochastic methods in Discrete Fracture Networks and a Coupled Processes Modeling Framework

Arezki Chabani[1*], Ghislain Trullenque [1], Rishi Parashar [2], Armand Pomart [1], Ruben Attali[1] and Ingo Sass[3]

[1] B2R, Institut Polytechnique UniLaSalle Beauvais, Geosciences Department, 19 Rue Pierre Waguet, F-60026 Beauvais, France
[2] Division of Hydrologic Sciences, Desert Research Institute, 2215 Raggio Parkway, Reno, NV 89512, United States
[3] Technische Universität Darmstadt, Institute of Applied Geosciences, Schnittspahnstraße 9, D-64287 Darmstadt, Germany

*Corresponding author: arezki.chabani@unilasalle.fr

Keywords: Enhanced Geothermal System (EGS), Reservoir analogue, Photogrammetric models, Discrete Fracture Network (DFN) Models, Fluid flow simulation

ABSTRACT

The MEET project (Multidisciplinary and multi-context demonstration of EGS exploration and Exploitation Techniques and potentials) is an interdisciplinary study aiming at the improvement of Enhanced Geothermal System (EGS) technology across Europe. The present work contributes to the MEET project in the form of a 3D structural model and Discrete Fracture Network (DFN) analysis, coupled with multi-physics models along key transects, of an analog for the Soultz-sous-Forêts reservoir (Upper Rhine Graben, France). The Noble Hills (Death Valley CA, USA) are chosen as analog due to the common transtensional tectonic setting (rifting zone), an arid region of near total outcrop exposure and making it ideal for Structure from photogrammetry images. In comparison to the Soultz-sous-Forêts reservoir, the Noble Hills has a similar granitic lithology, which has been fractured and hydrothermally altered. The front of the range is bounded by the Southern Death Valley Fault Zone (SDVFZ), a regional dextral fault, which places Tertiary sediments against granite. The photogrammetric models were produced from a combination of ground-based, unmanned aerial vehicle (UAV), and aerial photography. This multi-scale approach of image collection provided resolutions ranging from cm to dm scale. Planar feature extraction and detection was conducted using a combination of multi-point analysis, automatic facet detection, and manual polyline extraction. This planar data was extrapolated to construct a geometric model of the Noble Hills fracture network and ultimately create a representative 3D DFN model. Given the range of fracture size and relative complexity of fracture network, we implemented multiple workflows to address different aspects of the methodology. The DFNs were generated in 3D using a deterministic approach and the fracture planes were further projected onto orthogonal 2D slices for computing flow through interconnected network of fractures.

In total, 13 models are retained for the fluid flow simulations, localized along the major faults which structure the Noble Hills analog. The number of polylines extracted from the models is comprised between 318 to 7207 fractures. The variability in the number of fractures is related to the difference of the deformation gradient between the south and the north part of the Noble Hills.
The preliminary fluid flow simulations resulting from the Noble Hills models allow us to understand the interaction between the fracture geometry and stress field. Temperature is one of the main parameters of each hydrothermal system, and must be included to the models.

1. INTRODUCTION

Fracture systems characterization has become one of the most popular research topics in recent years inspired by CO_2 storage (Agosta et al., 2008), water resources (Mayer et al., 2007), nuclear waste storage (Rempe, 2007) and optimization of the resource concerning petroleum and geothermic reservoirs (Chabani et al., 2020; Géraud et al., 2015). Despite numerous studies, there is still the need for developing more geothermal projects to enhance the comprehension of the hydrothermal systems.

The MEET project (Multidisciplinary and multi-context demonstration of EGS exploration and Exploitation Techniques and potentials, (Trullenque et al., 2018)) is aiming at developing geothermal exploitation at European scale by applying Enhanced Geothermal System (EGS) technology to various geological settings. This ambition is challenging due to the variability of both structural settings and nature of rocks found on this continent. All commercially interesting geothermal reservoirs rely on the presence of heavily fractured rocks that permit fluid circulation up to surface installations (Fan and Parashar, 2019). A precise characterization of this fracture network at large scale is therefore of primary importance for the estimation of possible fluid flow rates and planning of future production sites.

Fracture modeling has been one of the most common topics developed in the recent years by many authors (Bonnet et al., 2001; Bour et al., 2002; Davy et al., 2010). The main goal is to enhance the comprehension of the fractured system spatial distributions in order to better understand the geometry of fluid circulation at the reservoir scale. Many authors performed fracture modeling using discrete fracture network (DFN) methodology (Bonneau et al., 2013, 2012; Bonnet et al., 2001; Borghi et al., 2015; Bour et al., 2002; Davy et al., 2006; Hardebol et al., 2015). This approach is either based on 1) stochastic, or 2) deterministic fracture generation. The stochastic method consist on simulation of fracture network by heuristic rules based on 1) mechanical principles (Bonneau et al., 2013), 2) fracture growth with opening mode, and 3) statistical distributions of fracture attributes (Bonnet et al., 2001; Bour et al., 2002; Davy et al., 2010; Priest, 1993; Priest and Hudson, 1981). Up to now, the input parameters of the stochastic models are based on statistic field measurements (Bonneau et al., 2013; Dershowitz et al., 1993; Xu and Dowd, 2010). Furthermore, the modeled fracture network are randomly distributed using the Poisson process method (Chiu et al., 2013), meaning that the modeled fracture positions do not correspond to the real position in the field.

The deterministic approach (Darcel et al., 2003) is based on the geometrical fracture parameters measured directly in the field. On one hand, this method presents a clear advantage in being representative of real fracture geometry, but, on the other hand it suffers from sampling bias. Small fractures are indeed underestimated as a vast majority of them are usually not measured by the geologist

(see Bonnet et al., (2001) for further explanations). In the present study, we propose to combine the stochastic and the deterministic approaches to better reflect the fracture network distribution modeled in the field by 1) digitalizing the fractures from photogrammetric models and creating the fracture network by deterministic approach, 2) extrapolate in space by stochastic algorithm the fracture network in order to reduce the sampling bias occurred during the fracture extractions.

The present work aims at gaining a large-scale visualization of a 3D fracture network in a granitic geothermal reservoir. Here, we present : 1) a methodology of fracture extrapolation from photogrammetric 3D models, 2) a technique to construct DFN models, 3) results of the DFN model's construction, and 4) preliminary results of flow simulation in 2D slices from the previously created DFN model. The purpose of the project is to calibrate the three-dimensional models built from the analogs and to compare the results with the actual Soultz-Sous-Forêt (Ssf) reservoir evolution.

2. GEOLOGICAL AND STRUCTURAL CONTEXT

We have chosen to investigate a fractured granitic basement paleo geothermal analog situated at the Southern termination of the Death Valley National Park (California, USA). Klee et al., (2020) (this volume) have investigated in depth the southernmost part of the Death Valley region and confirmed the analogy with Soultz-sous-Forêts reservoir. These authors argue that many similarities, notably 1) the granitic nature and alteration of the central portion of the NH, and 2) the transtensional tectonic setting of the DV region permit to consider the NH as an excellent analogue of the Soultz-sous-Forêts (SsF) reservoir. Considering the desertic conditions, the NH range is perfectly suited for realistic large-scale fracture network reconstructions and numerical flow simulations dedicated to the global understanding of fluid circulations in granitic reservoirs affected by extensional tectonics (Trullenque et al., 2018).

The Death Valley region contains a complex structural and tectonic history which includes the overprinting of Mesozoic to early Cenozoic contractional structures by late Cenozoic extensional and transtensional features (Miller and Pavlis, 2005; Pavlis et al., 2014; Snow and Wernicke, 1989). The northwest trending contractional structures of the Death Valley region have been estimated to have ceased by no later than 70 Ma and to have begun no earlier than 100 Ma, in line with the timing of the Sevier orogenic belt (DeCelles, 2004; Walker et al., 1995). More recent work, however, has uncovered evidence of an older sequence of northeast trending thrust faults in the region (Pavlis et al., 2014). Along with the development of contractional structures the Mesozoic also marked the beginning of pluton emplacement in the Death Valley region as part of the larger arc magmatism of the eastern Sierran Arc system (e.g. DeCelles, 2004). The late Cenozoic marked the beginning of extension in Death Valley, the earliest of which is recorded by the southwest directed Kingston Range-Halloran Hills system. This detachment system is constrained to a minimum age of 16 Ma and ceased movement by ~12.5 Ma, based on cross-cutting relations with the Kingston Peak granite (Calzia and Ramo, 2005; Calzia and Rämö, 2000). Following the Kingston Range detachment extension broadly shifted to the northwest, however, the magnitude and style of extension is not agreed upon, with some supporting a large-scale detachment fault (e.g. Holm and Wernicke, 1990; Snow, 2000) while others suggest a discrete fault model (e.g. Miller and Pavlis, 2005). Nevertheless, following the middle Miocene it is generally agreed upon that the regional deformation shifted to a predominately transtensional regime and the opening of the main Death Valley as a "pull-apart" basin beginning at ~5 Ma (Brady, 1987; Norton, 2011; Pavlis et al., 2014). According to Pavlis and Trullenque, (Submitted), the dextral displacement along the Death Valley fault zone are estimated about 40-41Km.

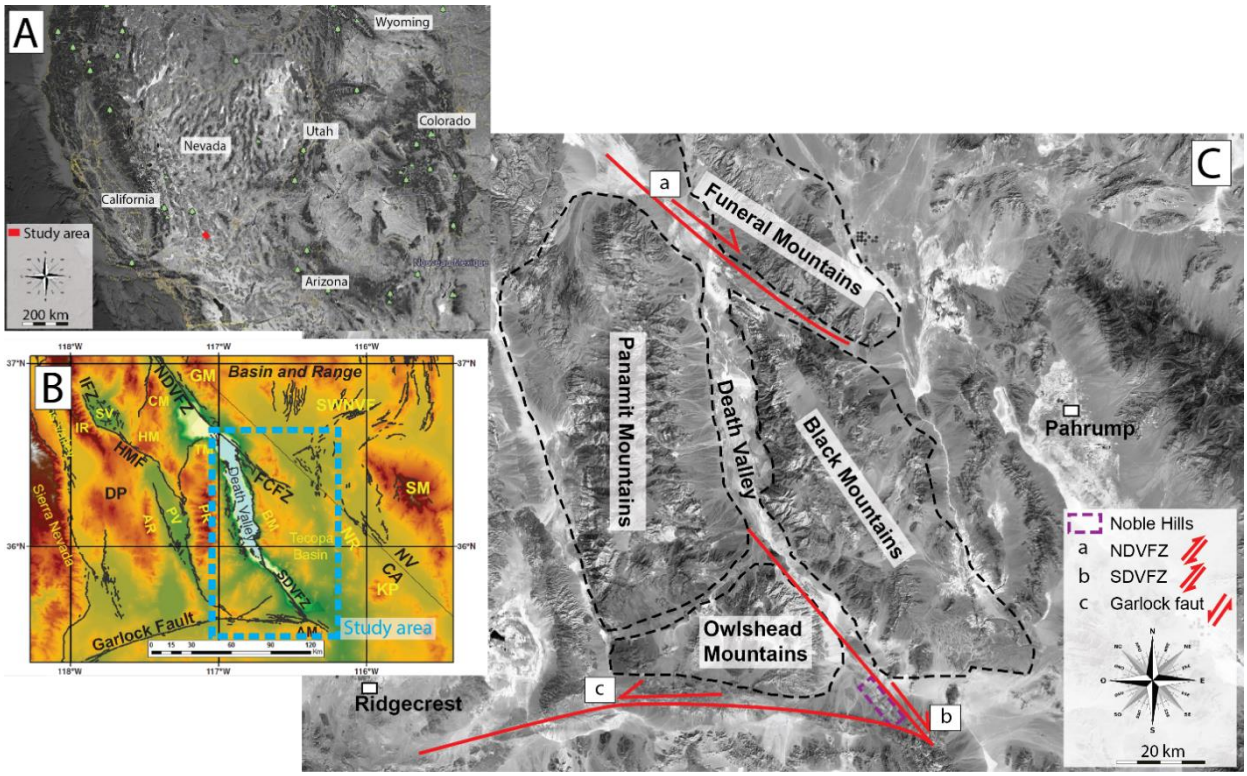

Figure 1: A, B: Location and geological setting of Death Valley (Norton, 2011). C: Tectonic domains (modified after (Norton, 2011). NDVFZ – Northern Death Valley Fault Zone; SDVFZ – Southern Death Valley Fault Zone.

3. DATA ACQUISITION AND PROCESSING

A photogrammetric campaign was performed within the NH in order to create a 3D realistic model of these outcrops using the Agisoft Metashape software (AgiSoft Metashape Professional. (2020), Version 1.6.5). Retrieved from http://www.agisoft.com/downloads/installer/. Then, the resulting fracture network can be extracted with CloudCompare (CloudCompare (version 2.9.1) [GPL software]. (2017). Retrieved from http://www.cloudcompare.org/ and extrapolated into Move suit (Move, Fracture modelling plugin (version 2019.1.7). (2019). Retrieved from https://www.petex.com/products/move-suite/fracture-modelling/, to further investigate of fluid flow through the fracture network.

3.1 Photogrammetric data acquisition

Two photogrammetric campaigns were carried out in October 2018. The former used a small aircraft flying through the Noble Hills to have an overview of the whole area. Photographs were taken around every 3 seconds between the late morning and early afternoon using a DSLR camera. Two drones (DJI Phantom 4 and 3DR Solo) with 4k cameras have been used to have representative cross sections that focus on the bounding fault zones and the fractured granitic bodies. The videos were recorded for 7 days and comprising 12 flights (including the plane flight) (figure 2). Pictures were then extracted every second from videos using ffmpeg software. The areas covered during the photogrammetry campaigns are localized sideways the major faults that structure the Noble Hills (faults in red lines on figure 2). The fault system is mainly striking NW/SE, following the structural orientation of the Noble Hills. The north part corresponds to the area covered by the Day 5 and 6 photogrammetry campaign, while the south part corresponds to the area covered by the days 1, 2, 3, and 4 (figure 2).

During the data acquisition period, three factors affect vastly the accuracy of later 3D realistic models. The first is the resolution of images and videos. Higher the resolution is, more points can be extracted, better are the 3D models. Nowadays, it is fully recommended to take pictures instead of videos during the photogrammetric campaign. Indeed, the resolution of pictures extracted from videos are severely impacted. The second is the overlapping of the pictures. The overlapping between two pictures must be at least of 60 % to insure a perfect merging. Furthermore, A support tool is fully recommended to stabilize the camera. To construct a 3D model from a set of pictures, the camera position for each picture needs to be determined correctly by using common points extracted from the overlapping part of several pictures. The third is the lighting condition that influences the picture color. It is difficult to identify the same point from two pictures with different color gamut. To reduce the effects of lighting condition, it is recommended to use the camera in manual mode to preserve the homogeneity of colors and light. Finally, the sky influences the 3D model construction by creating noises around the common points. In this sense, a new python script was developed and discussed below.

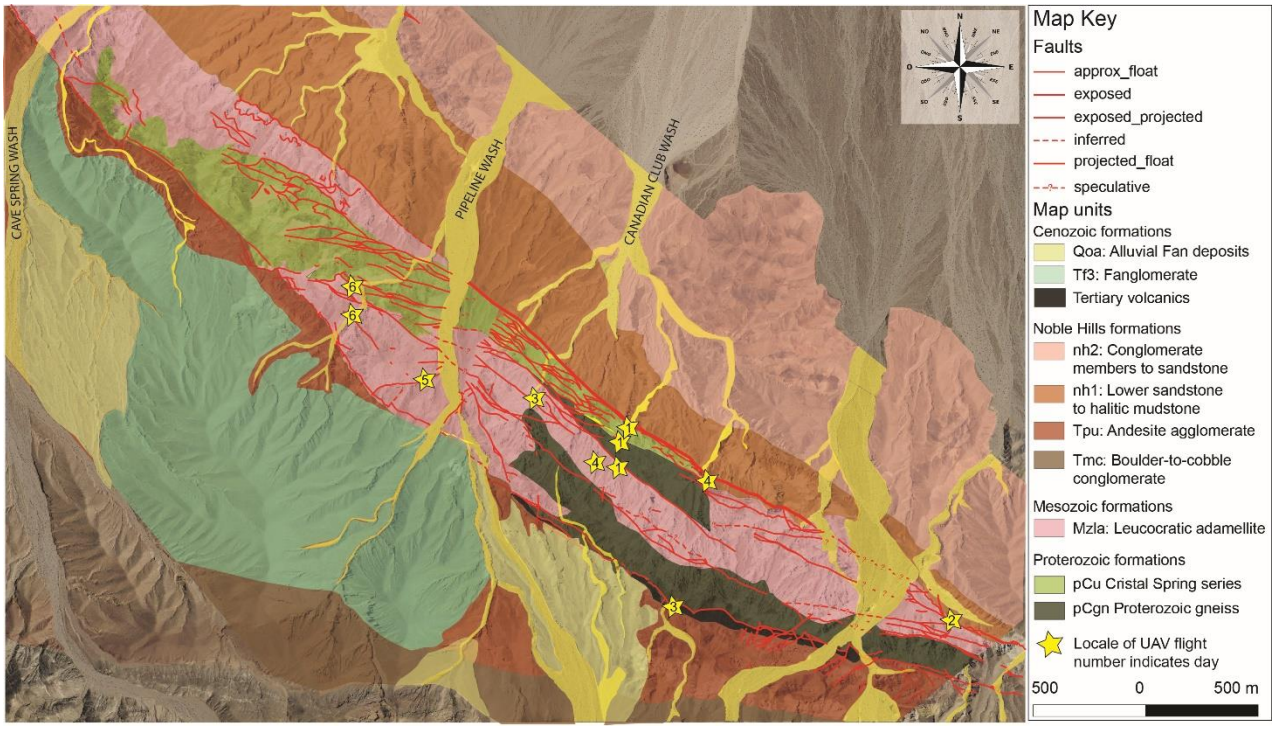

Figure 2: Position of the drone flights on the geologic map of studied area (modified after Klee et al., (2020) and Niles, (2016).

3.2 Photogrammetric processing

From acquired data, 3D realistic models were constructed by Agisoft Metashape software using Structure from photogrammetry method. General steps are summarized in the figure 3 and detailed below:

- **Pictures Chunks creation**: Creation of different pictures chunks from different flights (a canyon/outcrop can have more than one chunk.
- **Sky removal**: During the photogrammetric data acquisition, the sky constitutes at least 30 to 40% of some exposed pictures and thus create noises during the alignment process. A new python script has been implemented for this study in order to remove the sky. In a first step, a mask of bright objects is constructed, which should contain the sun, if present on the image,

as well as possible white structures of the image. This is done by selecting pixels with a value of more than 90% the maximal value (255 for JPEG images, 1 for PNG images) in the three channels, red, green and blue.
A second mask, of blue objects, is constructed in order to have a rough estimation of sky segmentation. First, the blue/red ratio of the image is computed, by dividing the blue channel of the image by the red channel (adding a small positive constant in order to avoid division by zero). A threshold "t" is estimated as the first minimum in the histogram of values of the ratio image between 1 and 2. Thresholding the blue/red ratio image over this value t provides the second mask.
Both masks are combined in order to form a first rough segmentation of the sky and sun. The postprocessing consists in computing the geodesical reconstruction of the first line of the image under this mask (in other words, only the connected components of the mask at the top of the image are kept. The mask is finally completed if necessary: if a pixel belongs to the detection mask, we add all pixels between it and the top of the image.
At the end of the process, a mask has been created for each analyzed picture and then added to the picture's chunks.

- **Pictures alignment**: Automatic alignment of pictures have been realized according to the following settings: high accuracy: Key Point Limit = 60.000 and Tie Point Limit = 0 (no limit). All of these settings are selected per defaults. In the advanced settings, masks related to the sky removal need to be applied to the Tie Point.
  In some cases, pictures are not aligned automatically. This is due to the insufficient overlapping between the two aligned pictures. Manual alignment option can be used to complete the pictures alignment (utilization of the Optimize function after each alignment). However, the manual alignment needs to be used with care because it can create several scattered common points and then impact the model quality.
- **Sparse point cloud**: A sparse point cloud containing millions of points (between 1 and 60 million) was generated. These points are situated on at least two different pictures. However, most of them had a significant error. Hence, it is necessary to eliminate those error points to obtain a high-resolution 3D photogrammetric model. Based on several trial tests, we have retained the following settings: Reconstruction uncertainty ≤ 10%, Projection accuracy ≤ 3%, Reprojection error ≤ 0.3%, Image count = 2. The Optimize function was also used after each error removal. After this step, more than 50% of the points are deleted. These settings have been fixed after several tests on the Death Valley models used in this study and may change in other cases due to the picture's quality acquisition and alignment.
- **Dense cloud model**: Construction of the dense point cloud with the following parameters: Accuracy = High, Depth filtering = Aggressive and Calculate point color ticked. The final model (dense point cloud) is composed of 30 to 200 million points. It corresponds to a few tens of thousands points from the sparse point cloud (generated in the previous step) and millions of points that are taken close to the previous points but only on pairs of pictures.
- **Export 3D model**: The 3D model can be saved into "Mesh" and then "Texture" which reflects a perfect contrast of the 3D relief (figure 4A). Then, the textured model can be exported into .TXT file to be used in CloudCompare software.

3.3 Georeferencing

First, the model of the Noble Hills (plane flight) was georeferenced. Indeed, 18 Ground Control Points (GCPs) were placed through the overflown zone with printed targets and their positions were measured with a Differential Global Positioning System (DGPS) (figure 3). The position of each GCP are corrected from with the standard deviation of the DGPS. Then, each GCP was selected and labelled on the photographs, directly on Agisoft Metashape, which makes the model georeferenced in the space.

Then, each chunk (drone flights) was aligned with the previous georeferenced model of the Noble Hills. Therefore, common points between both models must be manually chosen with the tool "Aligns two clouds by picking (at least 4) equivalent point pairs". At the end of the process, the model from the drone blend into the plane model and is georeferenced.

3.4 Fracture detection and extraction

Regional and local studies of linear features (eg. faults, joints, folds etc.) using satellite images, has made important progress in geological research during the last few decades (Rowan and Lathram, 1980). In addition, during the last few years, the photogrammetric and lidar images have made real advances in the understanding of the fracture patterns. The geometrical parameters of fractures at different scales, and of their importance on the field rock, rock physics, rock geophysics, and sectors of hydrogeology and energy and storage (Healy et al., 2017 and references therein). Then, a common set of tools have been developed to analyse and quantify the fracture patterns into 2D and 3D (Hardebol and Bertotti, 2013; Healy et al., 2017; Xu and Dowd, 2010; Zeeb et al., 2013). Hardebol and Bertotti, (2013) developed DigiFract software to work directly with fracture data from outcrops; Zeeb et al., (2013) developed FraNEP software which works only for a range of spatial sampling methods. The MATLAB™ FracPaq script developed by Healy et al., (2017) consists on a new toolbox, of MATLAB™ program conceptualized to quantify automatically fracture patterns. However, all of the software's and toolboxes can quantify the fracture patterns only in two dimensions (2D). Finally, the Facets CloudCompare plugin, developed by Dewez et al., (2016) can extract the geological planes automatically in three dimensions (3D). In the present study, we use the 3D facets plugin for the automatic detection and the Compass plugin for the manual detection of fractures from our 3D Noble Hills models.

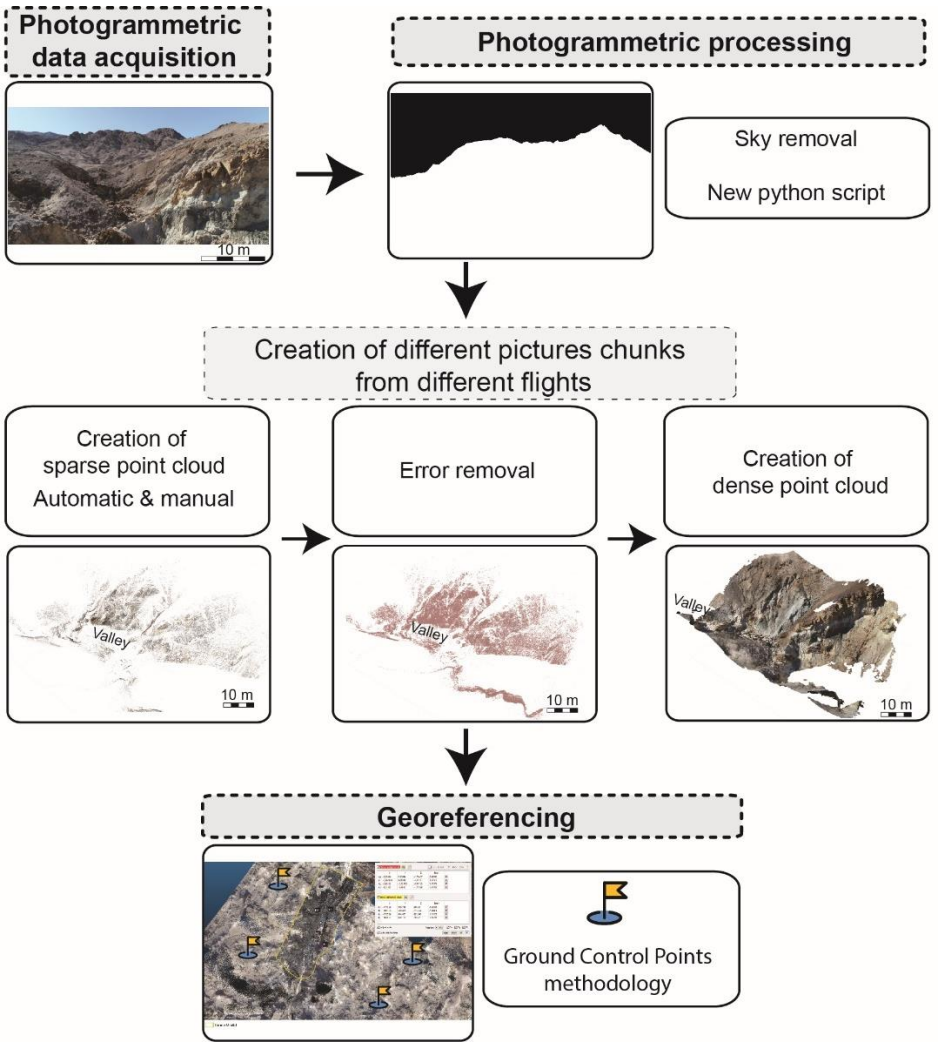

Figure 3: Workflow illustrating the different steps approved during the photogrammetric and the georeferencing processing.

As presented above, there are two possibilities to extract fractures from a point cloud: manually or automatically. The Compass plugin from CloudCompare lets the user manually trace fractures with either a 3D relief or a strong contrast (or both) (figure 4B, D), while the Facet plugin automatically fits 2D polygons to planar features (figure 4C, D). For each manual trace, a plane that best fit the polyline is created. For the automatic detection, the facets must be classified by orientation on well exposed outcrops with the Stereogram tool (figure 4E). Each facet family within 30° of strike and dip of each other is exported. This process is repeated for each family of fractures. But some facets exported in a set do not correspond to a fracture feature and must be deleted. The result of the above processing is a collection of facets and best fit planes to fracture traces which represent a 2.5D distribution of the fractures present within the point cloud model. In this study, the Compass plugin are mainly used to extract fractures manually from the models instead of the Facet plugin in order to reduce the feature's interpretation errors. Finally, the fitted polylines extracted can be exported as CSV file to extrapolate them into real size in MOVE® software.

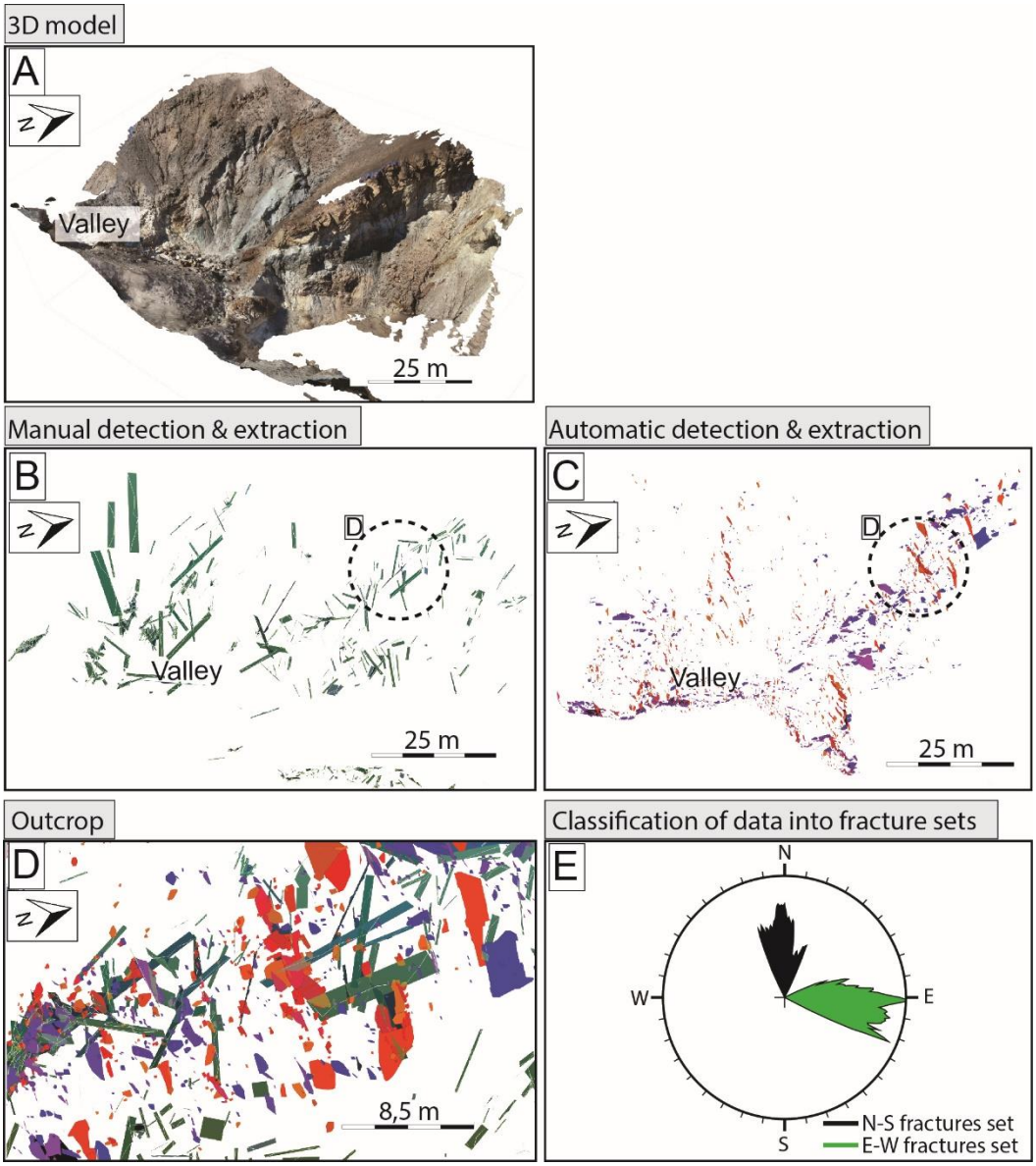

Figure 4: Process of fracture detection and extraction. A: 3D model obtained from aligned photos; B: Polylines and their planes extracted manually; C: Facets detected automatically. D: Geometry of the planes and the facets extracted/detected; E: Classification of the fracture network by orientation and size.

3.5 Fracture extrapolation

The extrapolation of the plane data exported from CloudCompare (Figure 5A) is a challenging task. The facet and best fit fractures only represent a small piece of the overall fracture and give an incomplete picture of the fracture's real geometry. First of all, we are not able to know how deep the fracture penetrate the sub-surface. Secondly, some fractures could be censored by vegetation or outcrop extend. In both cases, the extracted and measured fractures is underestimated. The fracture size (e.g. lengths) and density are two of the most difficult parameters to measure in the field, and then to model (Borghi et al., 2015). The deterministic and the stochastic approaches must be combined to build the most representative 3D DFN models, as described above. The first extracted fracture network studied here is obtained with the deterministic approach (figure 5A), based on genetic process of fracturation using a clustered point process around fractures identified from field (Bonneau et al., 2012; Srivastava et al., 2005). In the proposed methodology, the chosen Probability Density Function (PDF) for fracture length must be suited to the field observation.

Here we present a proposition of an extrapolation method from the fracture network extracted from CloudCompare. The first step is to bin the fractures by size with an increment of 0.5 meter (except for features above 8m², where the bin size is increased because these fractures are more like "real-world" fractures and mustn't be increased by this methodology to the risk of becoming unrealistic) (figure 5B). Then, the average aspect ratio is determined across all size ranges (the same work could be done on each separate bin to improve the methodology). A conservative methodology is therefore used to scale areas of the facet to the estimated "full size" fracture plan. It is based on the fact that fractures are supposed to be either ideal squares or circles. Furthermore, it is assumed that the facet or trace represents the diameter or side length of the "real world" fracture. Thus, the scaling factor is simply the ratio of a unit circle or square to a unit rectangle with the aspect ratio determined from the data. The .CSV data (that correspond to the facet and best fit planes) are imported to the software MOVE. The Create Surface Tool is used and a bin is chosen. Its width and height are set according to their bin size multiplied by the scaling factor. The method is repeated for each bin. It is finally converted to points to be used as input data for the creation of a fracture network model (figure 5C).

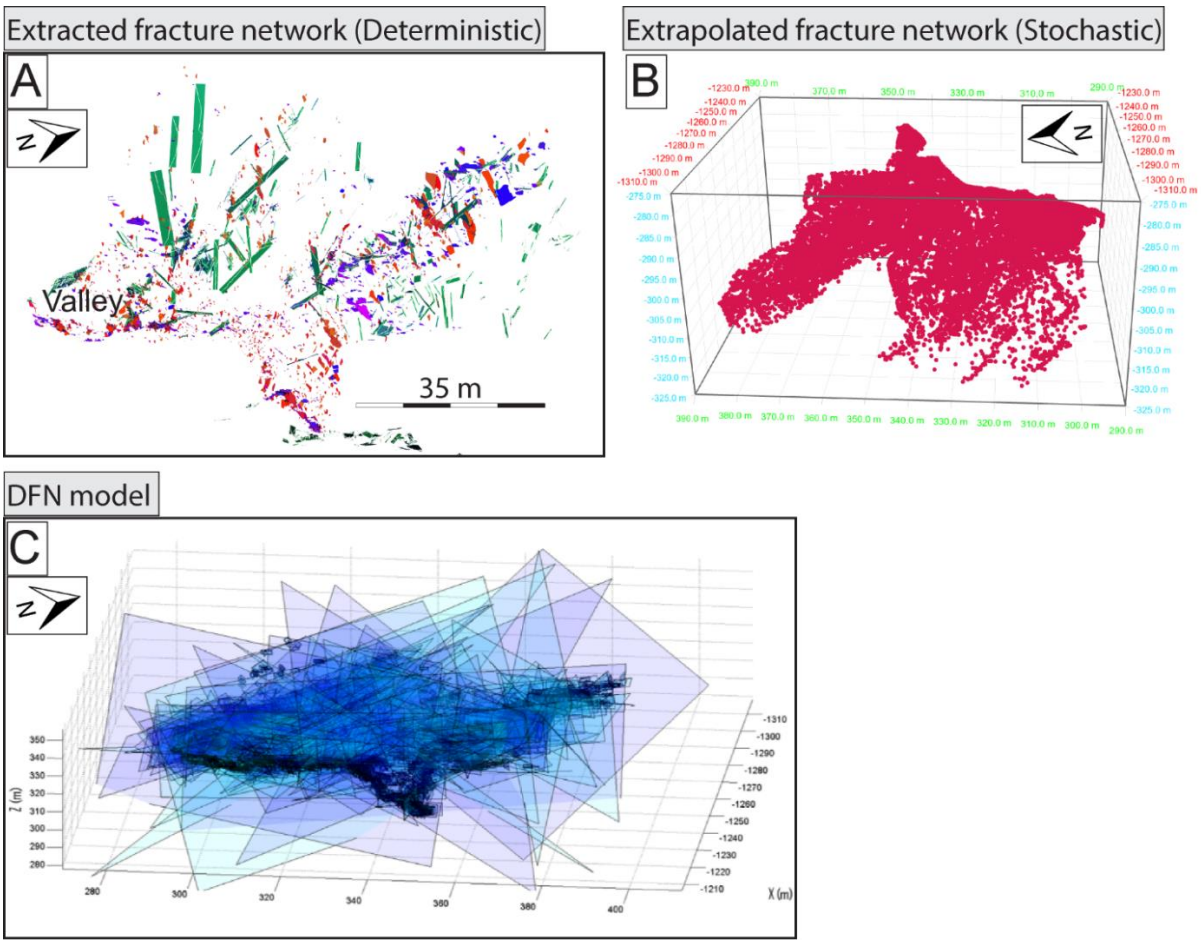

Figure 5: Process of extrapolation. A: Extracted fracture network from different models of the Death Valley analogue; B: Extrapolated fracture network to the real size using the stochastic method commonly used in DFN modeling; C: DFN model with the real size of fractures.

4. 3D FRACTURE NETWORK RESULTS

In total, 13 models are retained for the fluid flow simulations from the Noble Hills analog and are summarized in the table 1, which describes the statistical characteristics of each model. Note that, we tested the facets detection plugin only for the Day1C2. As described before, the facets detected should be corrected for the features which do not correspond to the fractures. The number of fractures extracted are highly variable according to the modeled area (table 1). Indeed, the number of fractures extracted from the Day 1 to Day 6 models (see the localization in the figure 2) are especially higher varying from 318 fractures (minimum extracted from the Day1C1 model) to 7207 fractures (maximum extracted from the Day2 models).

The two-dimensional fracture densities given by P21 parameter (see Holmen and Nils, (2002) for the explanation) for each area (table 1) show a high fractured area varying from 0.18 to 5.32 m/m² in the south part of the Noble Hills, while the P21 varies from 0.26 to 0.53 m/m² in the north part. In addition, the main fracture sets recorded in the Noble Hills are striking NW/SE (main fracture set) to NE/SE (second main fracture set) in the core part, and are striking NE/SW mainly in the north part. The evidences of the deformation gradient differences between the south and the north part of the Noble Hills which can explain the fracture densities differences are still to improve in the next publication.

Table 1: Statistical characteristics of 3D samples acquired from Noble Hills photogrammetrical models at the outcrop scale.

Day	Drone model (chunk)	Aligned Cameras	Tie point after processing	Dense cloud	Number of facets detected	Number of planes extracted	Surface densities (m/m²)	Main fracture sets
1	C1	813/818	148 026	90 951 617	0	318	0.18	NW/SE N/S
	C2	1117/1153	443 470	151 052 414	27 868	2209	0.48	NE/SW
	C3	254255	267 732	55 256 365	0	820	0.29	Heterogenous
2	C4	1252/1272	623 002	139 469 918	0	7207	3.24	NW/SE
	C5	1319/1326	474 390	157 478 877	0			NW/SE NE/SW
	C6	1272/1279	359 473	110 145 781	0			NW/SE
3	C7	766/839	410 955	199 097 917	0	4081	1.59	Heterogenous
3_Jim	C8	1637/1778	60 223	49 812 442	0	936	0.21	Heterogenous
4	C9	1178/1179	1 710 556	161 243 115	0	4808	3.70	NW/SE
	C10	892/1027	1 202 910	9 315 953	0	806	5.32	NW/SE
5	C11	3502/3776	70202	86 340 758	0	2229	0.03	NE/SW
6	C12	2180/2289	106669	89 479 444	0	1400	0.26	NE/SW NW/SE
	C13	1712/1738	138 989	124 080 721	0	2093	0.53	NE/SW NW/SE

The Noble Hills models have to be tested now from the water transmittivity by considering the connectivity of each modeled fracture network. In the section below, we discuss the different numerical simulations conducted on a test site located the Noble Hills.

5. DISCRETE FRACTURE NETWORK (DFN) MODEL

Fractured rock aquifers have high transmissivity and low storativity as water can be easily transmitted to a pumping well but the fracture themselves can store very little water. Interconnected networks of fractures exhibit strong multi-scale variability in geometric and hydraulic properties (e.g., de Dreuzy et al., 2001; Neuman, 2008, 2005; Painter et al., 2002; Parashar and Reeves, 2012; Reeves et al., 2012). The degree of fracture connectivity plays a major role in how fracture networks transmit water (e.g. Darcel et al., 2003). Of the approaches to solve for flow and transport through fractured rocks (Hadgu et al., 2017; Sahimi, 2011), DFN modeling approach has advanced significantly with the increase in computational power and the wide availability of high-performance computing systems. The DFN explicitly represents individual fractures. It assumes the rock matrix is impermeable and fluid flow can only occur through a connected fracture network (de Dreuzy et al., 2012; Dershowitz et al., 1993; Erhel et al., 2009; Hyman et al., 2015; Parashar and Reeves, 2012; Pichot et al., 2012; Reeves et al., 2013). Discrete fracture network approaches are favored in mechanistic studies because the local density of fracture networks is rarely sufficient for the representative elementary volume criterion to be satisfied, and traditional approaches of assigning an equivalent conductivity tensor and porosity to continuum grid cells tend to overly homogenize the representation of networks (Berkowitz, 2002; Hadgu et al., 2017; Klimczak et al., 2010; Neuman, 2008, 2005). By including a detailed geometric representation of the connectivity structure, DFN models allow for more accurate predictive simulations of flow and transport through fractured rocks.

The DFN models are computationally intensive and the central feature of the code is computation of flow in fracture segments, which in 2D results in a set of N linear algebraic equations of hydraulic head h (N being the total number of points at which two fractures intersect). The eigenvalues of such matrices are spread over several orders and lack the clustering necessary for the fast convergence of iterative techniques for linear systems (Parashar and Reeves, 2012). A two-dimensional DFN code built using the minimum residual method (MINRES) of solving large linear systems iteratively (Parashar and Reeves, 2012) is used here to conduct simulations for networks with a hypothetical well located in the center of the domain and pumping at a constant rate.

5.1. Numerical experiments with DFNs

Pattern of flow paths that forms in fractured rocks in response to water extraction from a pumping well has important implications for geothermal systems. If water flow paths from an injection well and/or from the surrounding rock matrix to a pumping well are limited to few dominant fracture segments, then the amount of heat captured is likely to be less than optimal. Conversely, if the fracture network characteristics promote dispersed set of path lines leading to a pumping well then it's likely to contribute to an efficient system for heat extraction. With the objective of understanding network connectivity patterns and flow path configurations in the extrapolated network obtained from the field campaign, we designed a pair of numerical experiments using 2D DFN tools.

A small 3D domain of 50 m x 50 m x 10 m was extracted from the fracture network produced from the Day 1 model (see the figure 2 for the location). The extracted network consists of a large percentage of small features (only a few meres in size) interspersed with few large features inducing strong connectivity in the system. This network becomes the basis of our first set of simulations. As it is

reasonable to expect that vast majority of small fractures were not detected during the field campaign, we construct a denser network by artificially adding smaller fractures with similar statistical properties to augment the network density by a factor of three. This denser network becomes the basis of our second set of simulations. Figure 6 shows both of these networks in 3D, and representation of fracture on orthogonal planes for construction of 2D DFN models. The 2D DFN in the horizontal (x-y) plane is used here to examine the influence of network connectivity on flow behavior.

The pair of numerical experiments were designed for the simple case of uniform aperture (500 microns) values of fractures in the network. Variability in aperture values will invariably lead to less dispersed flow and development of preferential pathways. The consideration of uniform apertures here is intended to serve as a starting point for evaluation of flow path dynamics in our system. The experiments were conceptualized with constant hydraulic head boundary condition on all four sides of the 2D model to study flow of water from surrounding volume of rock towards a pumping well. The dipole configuration of an injection well and a pumping well is computationally possible here but was not considered because of relatively smaller size of the model domain. A single pumping well was placed at the center of the model to extract water at a constant rate of 0.01 m^3/s (approximately 158 gpm). Steady-state flow solutions were obtained and flow path lines and hydraulic head drawdown were examined.

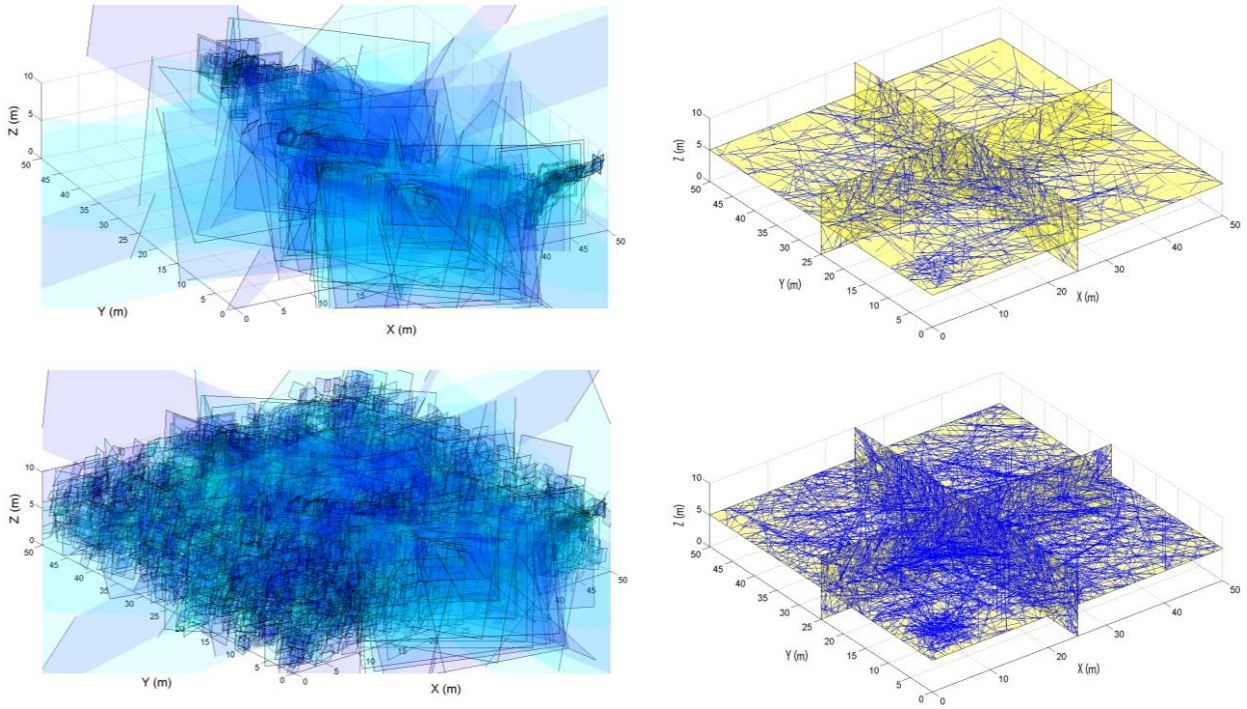

Figure 6: Numerically reconstructed fracture network in 3D (left column) and mapped traces of fractures on 2D orthogonal planes (right column). The top row only includes fractures identified from the field campaign. Fracture density in the bottom row is increased 3-fold by populating the domain with statistically similar smaller fractures.

Results of the DFN simulations are shown in Figure 7. It's immediately clear that the geometric attributes of fracture network are well suited for promoting strong connectivity. The relative flux values are seen to vary within a narrow range thus allowing extraction of water (and heat) from a large volume of surrounding matrix. This trend understandably becomes more pronounced when the density is augmented 3-fold by adding statistically similar smaller fractures to the model. The contour lines and cone of depression of hydraulic drawdown plots could be used as an ad-hoc to understand the expanse of area from which the pumping well draws water. Figure 7 shows a near symmetric (radially) drawdown pattern in the case of denser network and a slightly skewed pattern in the case of first network. These preliminary results suggest that the granitic fractured system studied here is aptly suited for geothermal resource exploration owing to the strong connectivity of fractures and associated dispersed patterns of flow behavior.

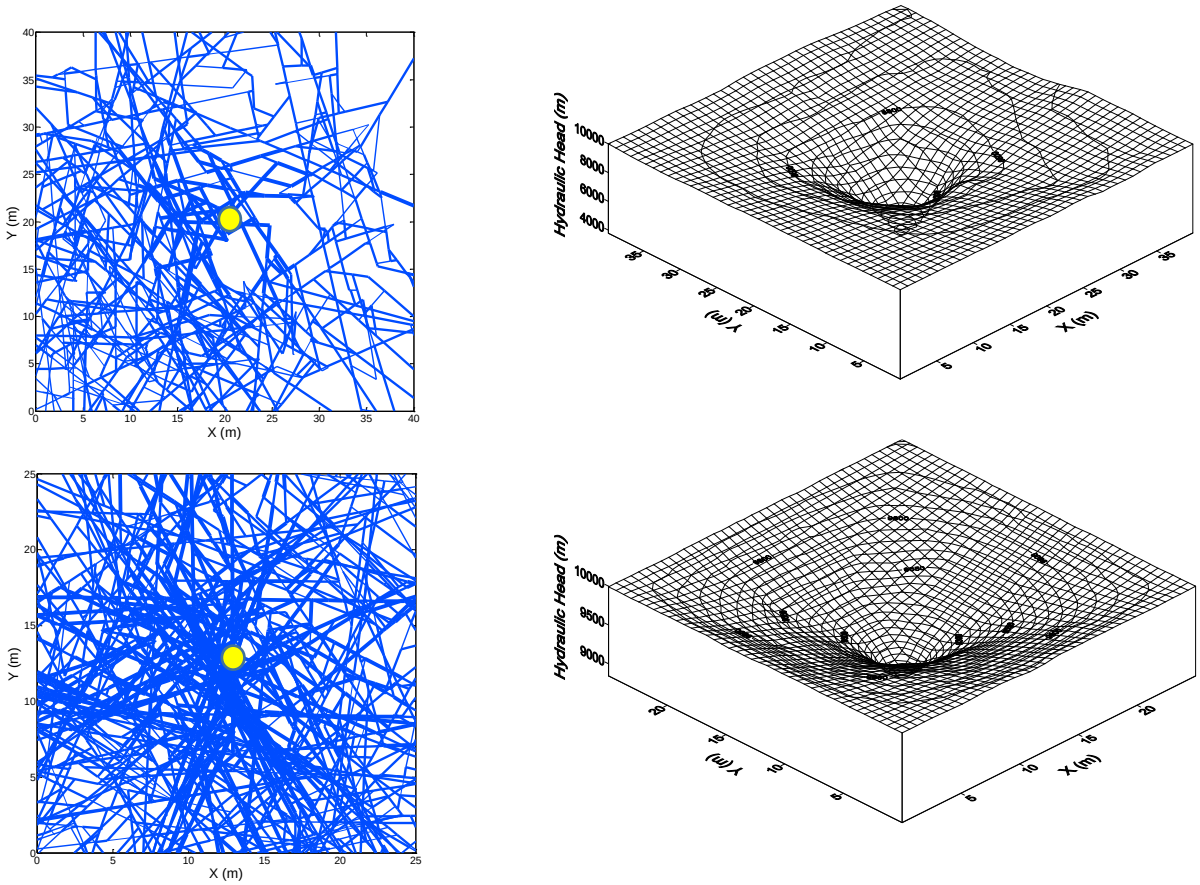

Figure 7: Solution of relative flux (represented by thickness of blue lines in the left column) and hydraulic head (right column) in response to pumping from a single well. The well location is shown by the yellow circle. The top row corresponds to the network constructed by using only the fractures identified from the field campaign, and the bottom row corresponds to the network with augmented (3-fold increase) fracture density.

6. CONCLUSION AND PERSPECTIVES

In this study, we present a new method to built a 3D DFN models from the Noble Hills range (Death Valley CA, USA), chosen as analogue of the Soultz-sous-Forêts geothermal reservoir. The following methodology is based on photogrammetric data taken by drone.

The 3D DFN realized here are based on multiscale approach, using a deterministic and stochastic methods. Combining the both methods bring a new approach to characterize the fracture systems at different scale, especially at reservoir scale. This multiscale characterization includes the length and spacing distributions, the fracture sets and densities. In total, 13 DFN models are constructed in the present study from the Noble Hills analog. The explanation for the difference between fracture densities recorded between the south and the north part of the Noble Hills is still to improve.

DFN simulations results from the 2D DFN slices highlighted a strong impact of the fracture density on the pressure drawdown. The selected trend become more pronounced when the density is augmented 3-fold by adding statistically similar smaller fractures to the model. This result still to approve in three dimensions at reservoir scale.

Fracture network models may be completed by additional studies as fractal analysis of the fracture network at different scales. This approach is based on characterizing fractures using law distributions (i.e power law and exponential law) and geometrical attributes of fractures. The purpose is to better understand the parameters which can control the fluid flow through complex fractured rock. Furthermore, temperature, stress field and fracture geometry parameters require to be considered in the fluid flow models to be able to compare the Soultz-sous-Forêts EGS site and similar geothermal systems.

AKNOWLEDGMENT

The presented results received funding from the European Union's Horizon 2020 research and innovation program under grant agreement No. 792037 (MEET). Prof. Terry Pavlis, Dr. José Hurtado, Dr. Zachariah Fleming, Dr. Mohammad Javad Afshari Moein and Johanne Klee are acknowledged for assistance in the field and fruitful discussions.

REFERENCES

Afshari Moein, M.J., 2018. Linkage between fracture network, stress heterogeneities and induced seismicity in deep geothermal reservoirs. ETH Zurich. https://doi.org/10.3929/ETHZ-B-000294223

Afshari Moein, M.J., Valley, B., Evans, K.F., 2019. Scaling of Fracture Patterns in Three Deep Boreholes and Implications for Constraining Fractal Discrete Fracture Network Models. Rock Mech Rock Eng 52, 1723–1743. https://doi.org/10.1007/s00603-019-1739-7

Agosta, F., Mulch, A., Chamberlain, P., Aydin, A., 2008. Geochemical traces of CO2-rich fluid flow along normal faults in central Italy. Geophysical Journal International 174, 758–770.

Berkowitz, B., 2002. Characterizing flow and transport in fractured geological media: A review. Advances in water resources 25, 861–884.

Bonneau, F., Caumon, G., Renard, P., Sausse, J., 2012. Stochastic sequential simulation of genetic-like discrete fracture networks.

Bonneau, F., Henrion, V., Caumon, G., Renard, P., Sausse, J., 2013. A methodology for pseudo-genetic stochastic modeling of discrete fracture networks. Computers & Geosciences 56, 12–22. https://doi.org/10.1016/j.cageo.2013.02.004

Bonnet, E., Bour, O., Odling, N.E., Davy, P., Main, I., Cowie, P., Berkowitz, B., 2001. Scaling of fracture systems in geological media. Reviews of geophysics 39, 347–383.

Borghi, A., Renard, P., Fournier, L., Negro, F., 2015. Stochastic fracture generation accounting for the stratification orientation in a folded environment based on an implicit geological model. Engineering Geology 187, 135–142. https://doi.org/10.1016/j.enggeo.2014.12.019

Bour, O., Davy, P., Darcel, C., Odling, N., 2002. A statistical scaling model for fracture network geometry, with validation on a multiscale mapping of a joint network (Hornelen Basin, Norway). Journal of Geophysical Research: Solid Earth 107, ETG 4-1-ETG 4-12.

Brady, R., 1987. Cenozoic geology of the Northern Avawatz Mountains in relation to the intersection of the Garlock and Death Valley fault zones, San Bernardino County, California.

Calzia, J., Ramo, O., 2005. Miocene rapakivi granites in the southern Death Valley region, California, USA. Earth-Science Reviews 73, 221–243. https://doi.org/10.1016/j.earscirev.2005.07.006

Calzia, J., Rämö, O., 2000. Late Cenozoic crustal extension and magmatism, southern Death Valley region, California. GSA Field Guides 2, 135–164.

Chabani, A., Mehl, C., Cojan, I., Alais, R., Bruel, D., 2020. Semi-automated component identification of a complex fracture network using a mixture of von Mises distributions: Application to the Ardeche margin (South-East France). Computers & Geosciences 137, 104435. https://doi.org/10.1016/j.cageo.2020.104435

Chiu, S.N., Stoyan, D., Kendall, W.S., Mecke, J., 2013. Stochastic geometry and its applications. John Wiley & Sons.

Darcel, C., Bour, O., Davy, P., de Dreuzy, J.R., 2003. Connectivity properties of two-dimensional fracture networks with stochastic fractal correlation: CONNECTIVITY OF 2D FRACTAL FRACTURE NETWORKS. Water Resour. Res. 39. https://doi.org/10.1029/2002WR001628

Davy, P., Bour, O., De Dreuzy, J.-R., Darcel, C., 2006. Flow in multiscale fractal fracture networks. Geological Society, London, Special Publications 261, 31–45.

Davy, P., Le Goc, R., Darcel, C., Bour, O., de Dreuzy, J.R., Munier, R., 2010. A likely universal model of fracture scaling and its consequence for crustal hydromechanics. J. Geophys. Res. 115, B10411. https://doi.org/10.1029/2009JB007043

de Dreuzy, J., Davy, P., Bour, O., 2001. Hydraulic properties of two-dimensional random fracture networks following a power law length distribution: 1. Effective connectivity. Water Resources Research 37, 2065–2078.

de Dreuzy, J.-R., Méheust, Y., Pichot, G., 2012. Influence of fracture scale heterogeneity on the flow properties of three-dimensional discrete fracture networks (DFN): 3D FRACTURE NETWORK PERMEABILITY. J. Geophys. Res. 117, n/a-n/a. https://doi.org/10.1029/2012JB009461

DeCelles, P.G., 2004. Late Jurassic to Eocene evolution of the Cordilleran thrust belt and foreland basin system, western U.S.A. American Journal of Science 304, 105–168. https://doi.org/10.2475/ajs.304.2.105

Dershowitz, W., Lee, G., Geier, J., Hitchcock, S., La Pointe, P., 1993. FracMan user documentation. Golder Associates Inc, Seattle.

Dewez, T., Girardeau-Montaut, D., Allanic, C., Rohmer, J., 2016. Facets: A cloudcompare plugin to extract geological planes from unstructured 3d point clouds.

Erhel, J., de Dreuzy, J.-R., Poirriez, B., 2009. Flow Simulation in Three-Dimensional Discrete Fracture Networks. SIAM J. Sci. Comput. 31, 2688–2705. https://doi.org/10.1137/080729244

Fan, Z., Eichhubl, P., Gale, J.F.W., 2016. Geomechanical analysis of fluid injection and seismic fault slip for the M_w 4.8 Timpson, Texas, earthquake sequence: GEOMECHANICS OF FLUID INJECTION TIMPSON. J. Geophys. Res. Solid Earth 121, 2798–2812. https://doi.org/10.1002/2016JB012821

Fan, Z., Parashar, R., 2019. Analytical Solutions for a Wellbore Subjected to a Non-isothermal Fluid Flux: Implications for Optimizing Injection Rates, Fracture Reactivation, and EGS Hydraulic Stimulation. Rock Mech Rock Eng 52, 4715–4729. https://doi.org/10.1007/s00603-019-01867-9

Gentier, S., Rachez, X., Ngoc, T.D.T., Peter-Borie, M., Souque, C., 2010. 3D flow modelling of the medium-term circulation test performed in the deep geothermal site of Soultz-sous-Forêts (France).

Géraud, Y., Bertrand, L., Le Garzic, E., Walter, B., Haffen, S., 2015. Multi-scalar analysis of the porous network for deep geothermal reservoir, input of the petrophysical properties of the fault zones. Proceedings World Geothermal Congress.

Hadgu, T., Karra, S., Kalinina, E., Makedonska, N., Hyman, J.D., Klise, K., Viswanathan, H.S., Wang, Y., 2017. A comparative study of discrete fracture network and equivalent continuum models for simulating flow and transport in the far field of a hypothetical nuclear waste repository in crystalline host rock. Journal of Hydrology 553, 59–70. https://doi.org/10.1016/j.jhydrol.2017.07.046

Hardebol, N.J., Bertotti, G., 2013. DigiFract: A software and data model implementation for flexible acquisition and processing of fracture data from outcrops. Computers & Geosciences 54, 326–336.

Hardebol, N.J., Maier, C., Nick, H., Geiger, S., Bertotti, G., Boro, H., 2015. Multiscale fracture network characterization and impact on flow: A case study on the Latemar carbonate platform. Journal of Geophysical Research: Solid Earth 120, 8197–8222.

Healy, D., Rizzo, R.E., Cornwell, D.G., Farrell, N.J.C., Watkins, H., Timms, N.E., Gomez-Rivas, E., Smith, M., 2017. FracPaQ: A MATLAB™ toolbox for the quantification of fracture patterns. Journal of Structural Geology 95, 1–16. https://doi.org/10.1016/j.jsg.2016.12.003

Holm, D.K., Wernicke, B., 1990. Black Mountains crustal section, Death Valley extended terrain, California. Geology 18, 520–523.

Holmen, J.G., Nils, O., 2002. Theoretical study of rock mass investigation efficiency.

Hyman, J.D., Karra, S., Makedonska, N., Gable, C.W., Painter, S.L., Viswanathan, H.S., 2015. dfnWorks: A discrete fracture network framework for modeling subsurface flow and transport. Computers & Geosciences 84, 10–19.

Klee, J., Trullenque, G., Ledésert, B., Potel, S., Hébert, R., Genter, A., 2020. Petrographic and Petrophysic Analyzes of Fractured Granites used as An Analogue of the Soultz-sous-Forêts Geothermal Reservoir: Noble Hills, CA, USA., in: Extended Abstract. Presented at the Proceedings World Geothermal Congress, Reykjavik, Island.

Klimczak, C., Schultz, R.A., Parashar, R., Reeves, D.M., 2010. Cubic law with aperture-length correlation: implications for network scale fluid flow. Hydrogeology Journal 18, 851–862.

Mayer, A., May, W., Lukkarila, C., Diehl, J., 2007. Estimation of fault-zone conductance by calibration of a regional groundwater flow model: Desert Hot Springs, California. Hydrogeology Journal 15, 1093–1106.

Miller, M., Pavlis, T., 2005. The Black Mountains turtlebacks: Rosetta stones of Death Valley tectonics. Earth-Science Reviews 73, 115–138. https://doi.org/10.1016/j.earscirev.2005.04.007

Neuman, S.P., 2008. Multiscale relationships between fracture length, aperture, density and permeability. Geophys. Res. Lett. 35, L22402. https://doi.org/10.1029/2008GL035622

Neuman, S.P., 2005. Trends, prospects and challenges in quantifying flow and transport through fractured rocks. Hydrogeol J 13, 124–147. https://doi.org/10.1007/s10040-004-0397-2

Niles, J.H., 2016. Post-middle pliocene tectonic development of the Noble Hills, southern Death Valley, California. (Doctoral dissertation). San Francisco State University.

Norton, I., 2011. Two-stage formation of Death Valley. Geosphere 7, 171–182. https://doi.org/10.1130/GES00588.1

Painter, S., Cvetkovic, V., Selroos, J.-O., 2002. Power-law velocity distributions in fracture networks: Numerical evidence and implications for tracer transport: POWER-LAW VELOCITY DISTRIBUTIONS IN FRACTURE NETWORKS. Geophys. Res. Lett. 29, 20-1-20–4. https://doi.org/10.1029/2002GL014960

Parashar, R., Reeves, D.M., 2012. On iterative techniques for computing flow in large two-dimensional discrete fracture networks. Journal of Computational and Applied Mathematics 236, 4712–4724. https://doi.org/10.1016/j.cam.2012.02.038

Pavlis, T.L., Rutkofske, J., Guerrero, F., Serpa, L.F., 2014. Structural overprinting of Mesozoic thrust systems in eastern California and its importance to reconstruction of Neogene extension in the southern Basin and Range. Geosphere 10, 732–756. https://doi.org/10.1130/GES00993.1

Pavlis, T.L., Trullenque, G., Submitted. Evidence for 40-41km of dextral slip on the southern Death Valley fault zone: Implications for Eastern California Zone and Extensional Tectonics. Geology.

Pichot, G., Erhel, J., de Dreuzy, J.-R., 2012. A Generalized Mixed Hybrid Mortar Method for Solving Flow in Stochastic Discrete Fracture Networks. SIAM J. Sci. Comput. 34, B86–B105. https://doi.org/10.1137/100804383

Priest, S.D., 1993. Discontinuity Analysis for Rock Engineering.

Priest, S.D., Hudson, J.A., 1981. Estimation of discontinuity spacing and trace length using scanline surveys. Presented at the International Journal of Rock Mechanics and Mining Sciences & Geomechanics Abstracts, Elsevier, pp. 183–197.

Reeves, D.M., Parashar, R., Pohll, G., Carroll, R., Badger, T., Willoughby, K., 2013. The use of discrete fracture network simulations in the design of horizontal hillslope drainage networks in fractured rock. Engineering Geology 163, 132–143. https://doi.org/10.1016/j.enggeo.2013.05.013

Reeves, D.M., Parashar, R., Zhang, Y., 2012. Hydrogeologic characterization of fractured rock masses intended for disposal of radioactive waste.

Rempe, N.T., 2007. Permanent underground repositories for radioactive waste. Progress in nuclear energy 49, 365–374.

Rowan, L.C., Lathram, E., 1980. Mineral exploration. Chapter 17, 553–605.

Sahimi, M., 2011. Flow and transport in porous media and fractured rock: from classical methods to modern approaches. John Wiley & Sons.

Snow, J.K., 2000. Cenozoic tectonism in the central Basin and Range; magnitude, rate, and distribution of upper crustal strain. American Journal of Science 300, 659–719. https://doi.org/10.2475/ajs.300.9.659

Snow, J.K., Wernicke, B., 1989. Uniqueness of geological correlations: An example from the Death Valley extended terrain. Geological Society of America Bulletin 101, 1351–1362.

Srivastava, R.M., Frykman, P., Jensen, M., 2005. Geostatistical Simulation of Fracture Networks, in: Leuangthong, O., Deutsch, C.V. (Eds.), Geostatistics Banff 2004, Quantitative Geology and Geostatistics. Springer Netherlands, Dordrecht, pp. 295–304. https://doi.org/10.1007/978-1-4020-3610-1_30

Tester, J.W., Batchlor, A.S., Blackwell, D.D., DiPippo, R., Drake, E.M., 2006. The future of geothermal energy. Presented at the Oversight hearing on Renewable Energy Opportunities and Issues on Federal Lands: Review of Title II, Subtitle B- Geothermal Energy of EPAct; and other renewable programs and proposal for public resources, Massachusetts Institute of Technology.

Trullenque, G., Genter, A., Leiss, B., Wagner, B., Bouchet, R., Léoutre, E., Malnar, B., Bär, K., Rajšl, I., 2018. Upscaling of EGS in different geological conditions: a European perspective, in: Procs. 43rd Workshop on Geothermal Reservoir Engineering.

Walker, J.D., Burchfiel, B., Davis, G.A., 1995. New age controls on initiation and timing of foreland belt thrusting in the Clark Mountains, southern California. Geological Society of America Bulletin 107, 742–750.

Xu, C., Dowd, P., 2010. A new computer code for discrete fracture network modelling. Computers & Geosciences 36, 292–301.

Zeeb, C., Gomez-Rivas, E., Bons, P.D., Blum, P., 2013. Evaluation of sampling methods for fracture network characterization using outcrops. AAPG Bulletin 97, 1545–1566.